

**MOSQUITONET: INVESTIGATING THE USE OF UNMANNED AERIAL
VEHICLES AND NEURAL NETWORKS FOR INTEGRATED MOSQUITO
MANAGEMENT**

A Thesis

Presented to the Faculty of the Graduate School

of Cornell University

In Partial Fulfillment of the Requirements for the Degree of

Master of Science

by

Elizabeth Hillary Case

December 2017

© 2017 Elizabeth Hillary Case

ABSTRACT

Integrated mosquito control is expensive and resource intensive, and changing climatic factors are predicted to expand the habitat ranges of mosquitos and other disease-carrying vectors into new regions within the United States. Currently, low-cost unmanned aerial vehicles (UAVs) can be used to photograph and map large areas at centimeter-scale resolution, and already are starting to be used by vector control personnel to efficiently locate mosquito habitat. However, post-processing of UAV images is still time intensive, often done manually, or with programs built for satellite imagery. Moreover, UAVs have never previously been used to assess habitat suitability in the more populated areas preferred by *Aedes albopictus*, a species that breeds primarily in standing water in artificial containers near human populations. This work explored the use of UAVs and convolutional neural for integrated mosquito management.

Two neighborhoods comprising 125 houses in a densely-populated area of southern New York, were surveyed over nine days in 2017 with an unmanned aerial vehicle (UAV). The UAV survey coincided with an entomological survey, which was conducted on a subset of the houses to establish the presence and distribution of mosquito species. 64% the of 629 containers surveyed on all properties could be seen from the UAV, with almost 2,000 more features were identified the images (e.g. from houses that were not surveyed). In total, more than 2500 objects of interest (containers suitable mosquito habitat or related features) were identified in the aerial photographs. Two previously-published neural network architectures were trained on this novel set

of UAV aerial imagery. Single Shot Multibox Detection was used for image segmentation, achieving an average precision of 59%, a recall of 35%, and an overall accuracy of 31%. Separately, a fully convolutional neural net based on the VGG16 architecture, initiated with ImageNet weights and finetuned on images of surveyed properties assigned as positive or negative for *Ae. albopictus* larvae, achieved a binary classification of 80%.

When combined with image segmentation neural networks, unmanned aerial vehicles show promise for identifying potential habitat for *Ae. albopictus*, increasing the ability of vector control personnel to manage mosquito populations. The neural networks' abilities to predict larval presence could be further advanced by expanding training datasets, especially where containers of interest may vary by neighborhood.

BIOGRAPHICAL SKETCH

Elizabeth Case received a Bachelor's of Science in Physics from the University of California, Los Angeles in 2014. She worked as a science and environmental journalist and bicycled across the country teaching science before starting her Master of Science program at Cornell University in 2015. She entered the doctoral program in Earth and Environmental Sciences at Columbia University in 2017 to study the polar regions in this rapidly changing world.

DEDICATION

Special thanks to all those who have helped me through this: my parents, Jan and Loyd, and my sister, Emily, for their encouragement, guidance and hours of brainstorming and practice presentations, Dave G., for your steadfast support and the many dinners, and Steve M., for your unwavering belief in my ability to do this work.

This work wouldn't be possible without you.

ACKNOWLEDGMENTS

This work was funded in part by the National Science Foundation's Graduate Research Fellowship (DGE-1650441), the Atkinson Center for Sustainable Development, and the National Institute for Health

TABLE OF CONTENTS

Background	1-3
Methods	
i. Mapping	3-4
ii. Entomological and Container Survey	4-5
iii. Data Processing	5-8
Results	8-14
Discussion	15-16
Conclusion	16-17
References	18-19
Appendix	
i. Construction of the drone	20
ii. Data sheet for property survey	21
iii. Full list of tagged items in aerial photographs	22

LIST OF FIGURES

Figure 1: Type and number of containers identified in aerial photographs	6
Figure 2: Workflow	7
Figure 3: Map of photographs and identified items in Neighborhood 2	8
Figure 4: Visibility of containers on all properties	9
Figure 5: Distribution of all containers and visibility of items shaded	10
Figure 6: SSD neural network performance on top 13 categories	12
Figure 7: Sample output from SSD neural network	13
Figure 8: Activation layer example from fully convolutional network	14

BACKGROUND

The public health risks of *Aedes albopictus* have been well documented outside of the USA as a major vector of chikungunya and secondary carrier of Zika and dengue [1], and within the country as a carrier of eastern equine encephalitis and West Nile virus. While transmission of exotic viral pathogens by mosquitos in the United States is rare, *Ae. albopictus* is expected to spread further into the populous northeastern regions, given changing climatic conditions, e.g. more temperate winters [2].

Ae. albopictus is a container-laying species [3] and an aggressive daytime biter that feeds readily on human hosts [4]. To minimize potential risk to humans, organized mosquito control is necessary for population monitoring and suppression. Yet, as new species expand their range, resource-constrained agencies struggle to adapt their protocols to the different breeding habits, life cycle needs and public health consequences of invading species. The best way to control *Ae. albopictus* is to remove local sources of habitat by draining standing water that accumulates in containers like flower pots, buckets, cans, trash piles, and tires [5]. Nevertheless, the monitoring and control of container breeding species can be an insurmountable challenge due to the time, labor and logistical barriers involved in inspecting enough domestic sites. While water dumping campaigns encourage residents to remove all standing water, it is difficult for mosquito control agencies to determine the efficacy of such interventions, or to monitor habitats that may occur in difficult-to-reach places that residents may not initially notice (e.g. clogged gutters, along property borders, etc) [6].

To facilitate the identification of *Ae. albopictus* habitat in suburban and urban neighborhoods, we investigated the usefulness of two emergent technologies: unmanned aerial vehicles (UAVs) and

artificial neural networks,. The incorporation of these technologies may help vector control agencies overcome some of the existing barriers to widespread, comprehensive monitoring programs.

While unmanned aerial vehicles have long been used for military operations and by hobbyists, they have exploded onto the consumer market in the last five years [7]. This proliferation has made them readily available and inexpensive enough for conservation and land management purposes, see for example Seymour, et. al [8] and Candiago, et. al [9]. Although high resolution satellite imagery like the Landsat or the WorldView series can be used to find large bodies of water and define individual properties, it has neither the temporal nor spatial resolution to track the small water-holding containers that *Ae. albopictus* prefer to deposit eggs in. As an alternative, commercially available UAVs, which can provide images at resolutions 1.5 centimeters or finer, offer the flexibility and precision required for comprehensive mosquito habitat monitoring. Indeed, UAVs have been used in relation to mosquitos to: 1) take aerial photographs of malaria infested regions [10]; 2) distribute agricultural pesticides [11]; 3) search for standing water[12] and take water samples [13]; and 4) identify incidences of urban water accumulation [14]. To the authors' knowledge, there has been no previously-published example of using UAVs to assess property risk for suitable mosquito habitats in suburban neighborhoods. Moreover, UAVs can record high resolution images of areas as large as 30-60 hectares in under an hour, using equipment that costs between US \$600 and \$1200.

However, the ability to quickly and easily capture hundreds or thousands of pictures per day means that data management and analysis can take the place of the obstacles encountered in traditional vector monitoring methods. One possible tool to make sorting and identifying UAV photographs more quickly is neural networks, which were invented in the 1950s and 60s [15],

but didn't emerge as promising tools for image classification purposes until the late 2000s. In particular, convolutional neural networks (CNN) have been highly successful at image recognition tasks, because their architectures allow them to traverse the image for location-invariant identification of objects. CNNs have been trained to accurately classify skin cancer [16] and satellite imagery [17] as accurately as trained doctors or technicians, among many other tasks.

In this study, each of the aerial photographs had many features of interest we wanted to identify. For image segmentation, we used the Single Shot Multibox Detection (SSD) neural network architecture [18], which is built on VGG16 [19]. SSD speeds up image detection tasks by pre-defining a set of bounding boxes, selecting for boxes that have objects of interest, and adjusting those bounding boxes to surround the objects. This image detection architecture was selected over others like YOLO [20] and OverFeat [21], because it defines bounding boxes at various resolutions, scales and locations. Although Liu et. al reported that SSD was less effective on small objects, compared with identification of large features, we determined this architecture was still the best fit for our dataset.

METHODS

Mapping

Two neighborhoods in Westchester (Neighborhood 1) and Suffolk (Neighborhood 2) counties in New York, USA were mapped on 21-23 July (Session 1), 4-6 August (Session 2) and 11-12 August 2017 (Session 3). The primary UAV used during Session 1 and most of Session 2 (referred to as "quadcopter") was built from readily available parts (more fully described in Appendix 1). The pilot (EHC) received a small UAS pilot license in 2016 and had about 50 hours of flight time before fieldwork began. The U.S. Federal Aviation Administration prohibits drones

from flying over (uncovered) people not part of the flight team and requires that the team maintain a line of sight with the drone at all times. [22] These were accomplished by planning routes that largely travelled over covered buildings, flying between the hours of 10 a.m. and 3 p.m. during weekdays with temperatures $> 30^{\circ}\text{C}$, so that residents would be inside or at work, and sending a visual observer to follow the drone and ensure no people were directly under the flight path. The visual observer kept in contact with the pilot at all times via cellphone.

Each path was 1-1.7 km in length; the neighborhoods ranged in size from 5 to 14 ha. Each battery on the quadcopter was sufficient for 6-8 minutes of flight, which covered about 4 ha and 20-30 houses. The drone was flown at an altitude of 40 or 50 meters relative to the take-off point at a max speed of 5 m/s; the slower the speed, the higher quality the pictures. The camera (Go Pro Hero 5 (Go Pro, Calif., USA)) was set to have shutter speeds of no longer than 1/800 s to ensure high image quality. Theoretical maximum ground resolutions for the Go Pro cameras are between 1.5 and 4 cm/pixel, depending on altitude; however, vibration and exposure time both affected image resolution.

The secondary quadcopter, used to take about 1/3 of the pictures from Session 2, and all of the pictures in Session 3, was a DJI Mavic Pro (DJI, China), which came on the market during the planning and building phase of the study. The Mavic Pro had better stability and vibration damping, which translated into higher resolution pictures. In addition, the Mavic Pro could fly for 20-25 minutes on a battery and cover 12+ hectares in a flight.

Entomological and Container Survey

An entomological survey was conducted on a subset of the houses in each neighborhood to determine the presence and distribution of mosquito species. Each container holding water was examined for larvae and pupae; these were collected for identification. The category and material

of the container was recorded, along with water temperature, water volume, plant presence, shading and other variables. All containers were photographed and geotagged. In the second and third rounds of surveying, all containers (total: 630) that could hold water – not just those that contained water at the time –were recorded to better understand what the UAV could and could not see. We also recorded whether the container was obscured from above, whether it had any water, and whether any of the survey team members were bitten by *Ae. albopictus* during the survey. See Appendix 2 for an example of the data sheet.

To link the ground-truthed photos and larval presence to the aerial surveys, we adapted PhotoGPS [23], to map the distribution of containers and aerial images.

Data processing

The images were processed in a series of steps for preparation for neural network classification and to better understand what the drone was able to see and what it missed in the aerial survey. All pictures were taken on a GoPro Hero5 or on the Mavic Pro, which both produced photographs with dimensions of 3000 x 4000 pixels. To the authors' knowledge, there were no comparable available datasets of UAV aerial imagery over suburban areas.

Because 12 MP images would generate too many parameters in the convolutional network, the images were sliced into segments and will be referred to as follows:

1. “Whole scene”: The outer 500 pixels were cropped to account for lens distortion with GO PRO photos. No shaving was done for DJI.
2. “Tiled scene”: Images were tiled to create as close to 512 x 512 or 500 x 500 pixel images as possible at full resolution
3. “Tagged scene”: Each image was sorted and any features annotated using the Labellmg [24] software to produce bounding boxes for the SSD net

In all, more than 12,000 cropped images were sorted, yielding 1080 tiled images with 2500+ features of interest in 47 categories, which included identified objects such as containers, buildings, and common household and yard items. The full set of features is listed in Appendix 3.

There were several difficulties encountered during identification and annotation. Chief among these were: shading that obscured features and blown out white balance that reduced definition of features and covered areas like awnings, umbrellas, and trees. Additionally, some of the labelling on property that was not ground-truthed was subjective, though we tried to be as consistent as possible. Some smaller containers were difficult to discern; this was somewhat mediated by having the image examined by two people. If both were more than 50% confident it was a container (e.g. capable of holding standing water), the container was marked. Some flower

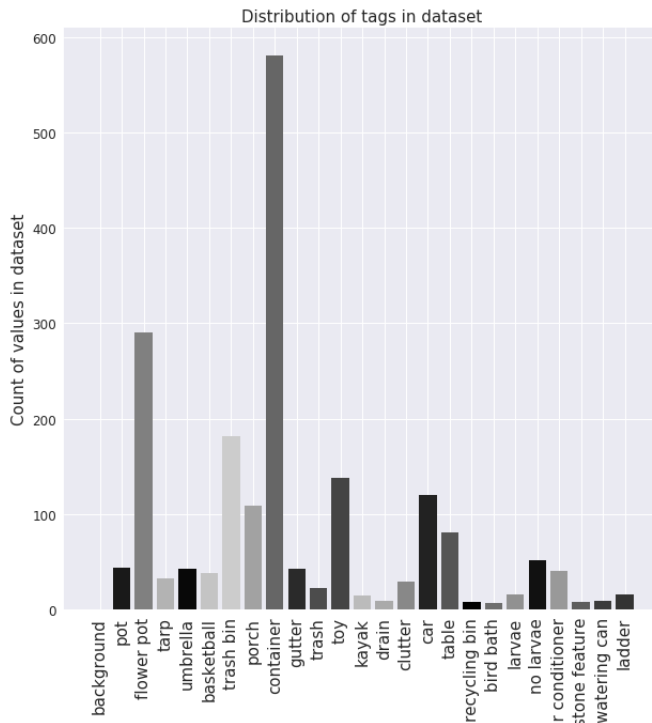


Figure 1: Distribution of categories in the training set from annotation of the aerial images for the image segmentation (SSD) neural network

pots and garbage bins were additionally labelled “containers”; other times they were not; this may have affected the precision of the neural network output by effectively assigning more than one label to a category of objects.

Because there was substantial overlap in each photograph, we were unconcerned about losing data through cropping;

additionally, not every feature of interest in every image was tagged, because some features were repeated multiple

times. In the final classification, 24 of the most prominent of these features were used. There were, for example, many more containers and flower pots than other features; see Figure 1 for object distribution in the training set. We did not attempt to address the imbalance in this paper; this is left for future work.

Additionally, each photo was manually annotated with the direction of travel of the UAV, which enabled us to convert each of the pixel locations of the images in the training, validation and test sets into GPS coordinates. This was done by hand for the Go Pro photos and translated from the Yaw information in the exif data of the DJI Mavic photographs.

The neural network was implemented in Keras (1.2.2) on top of Tensorflow (1.3.0) by Andrey Rykov [25], and initialized with ImageNet weights based on the original SSD300 implementation in Caffe. A second implementation by the original SSD authors, built for larger photographs (SSD512) would likely yield improved accuracy, especially for smaller items, but was not attempted in this paper. All computation was conducted on an Amazon EC2 p2.xlarge instance using an Amazon Machine Image from fast.ai [26]. The first 11 layers of SSD were frozen with the ImageNet weights and not fine-tuned on the aerial images because these layers have

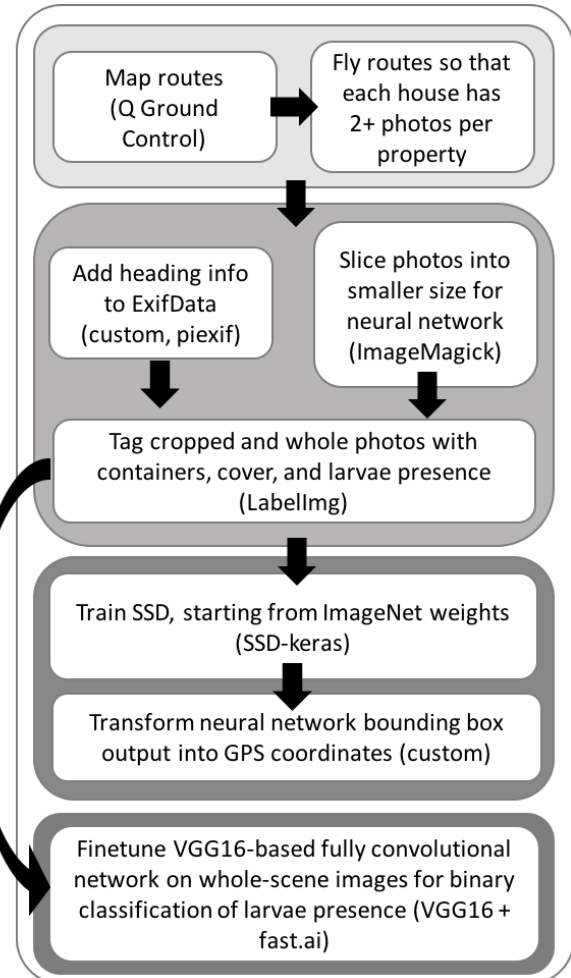


Figure 2: Workflow from image collection through neural network analysis, with packages/software used

been shown to activate on general features like grids and edges; moreover, our dataset was too small to train the full network. Images were augmented through random cropping, rotating, changes in brightness, and skew; this is standard and improves classification. Adam [27] was used for the optimizer; RMS-prop and Eve were tested but did not show improvement. The learning rate started at $1e-4$ and decayed by 10%, until the validation loss plateaued for three epochs, and then was reduced ten-fold, ending around $1e-7$. Overfitting became an issue within 25 epochs of fine-tuning, likely because the dataset is very small. See Figure 2 for an overview of our workflow.

RESULTS

As seen by the UAV

One of the unknowns in this study was how well containers of interest could be

identified from the aerial images because suitable mosquito habitat forms in containers under awnings, porches, tree cover, and elsewhere that is difficult or impossible to see from the air. Of

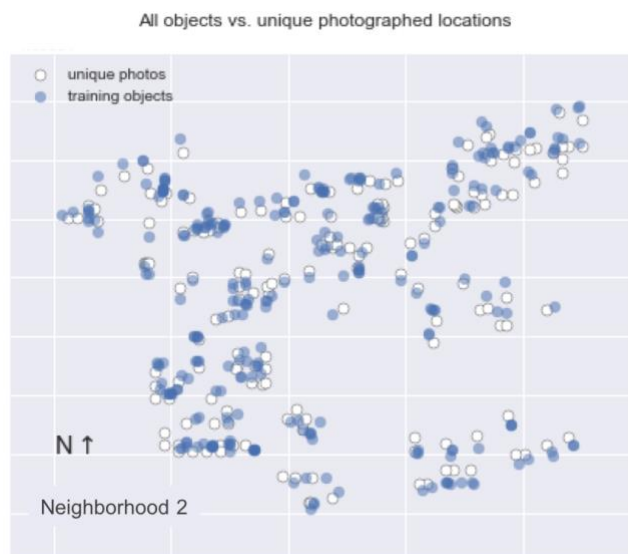


Figure 3: Distribution of a subset of photos taken (white dots) and objects identified within those photos (blue dots). GPS coordinates are not included to preserve the privacy of homeowners.

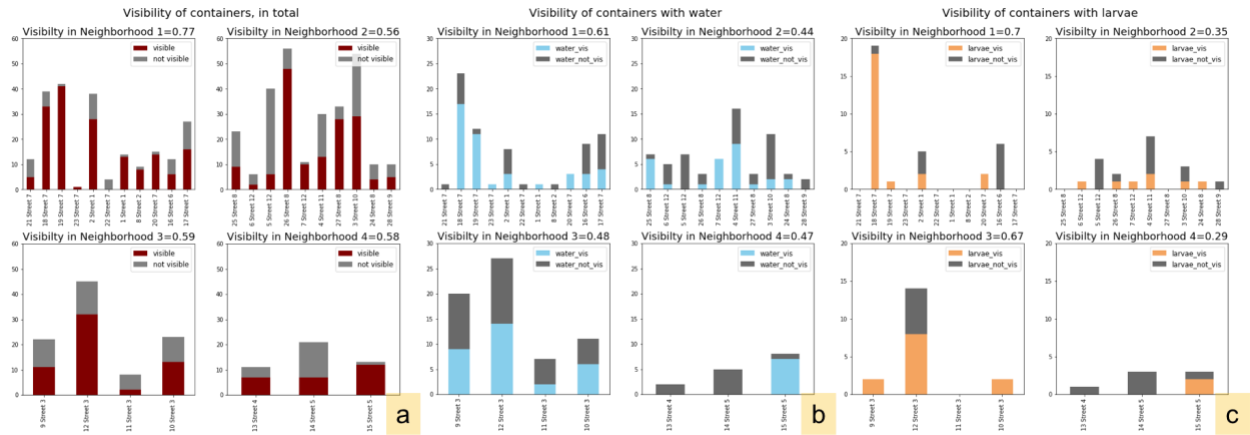


Figure 4: Visibility of containers from the drone changes depending on neighborhood and the features of interest – whether the container had water or larvae. Visibility in Neighborhood 1 was much higher than the other neighborhoods across both variables of interest, likely because the properties were wide and flat and had very little tree cover. The visibility of a container was estimated from the ground for all containers and confirmed from aerial images for containers with larvae; estimation and actual visibility was about 90%.

all containers surveyed on all properties, 64% of the containers were fully visible from the air,

and another 14% were partially visible. The location of the UAV over the property also

determined the ability to see

an object if it was close (within 2 feet) to house walls or other large objects. We also found that

visibility varied from neighborhood to neighborhood; almost 70% of the containers with larvae

in them were visible in Neighborhood 1, but only 35% of those containers were visible in

Neighborhood 2. Figure 3 shows a map of the photographs and items of interest in those

photographs in Neighborhood 2, and Figure 4 shows the visibility of containers from all ground

surveys from the air. Visibility depended strongly on neighborhood, which indicates that

environmental factors like tree cover may play a roll in the usefulness of UAVs for surveillance.

During the entomological survey for mosquito larvae in both neighborhoods over all three

weekends, we identified 134 containers that held water. Of these, 30 were not photographed

because there were people present on the properties at the time of the aerial surveys (a violation

of U.S. FAA Part 107). Of those that were photographed, 41 could be seen in the images, 45

could not be seen (10 potentially could have been seen if photographed at a different angle or

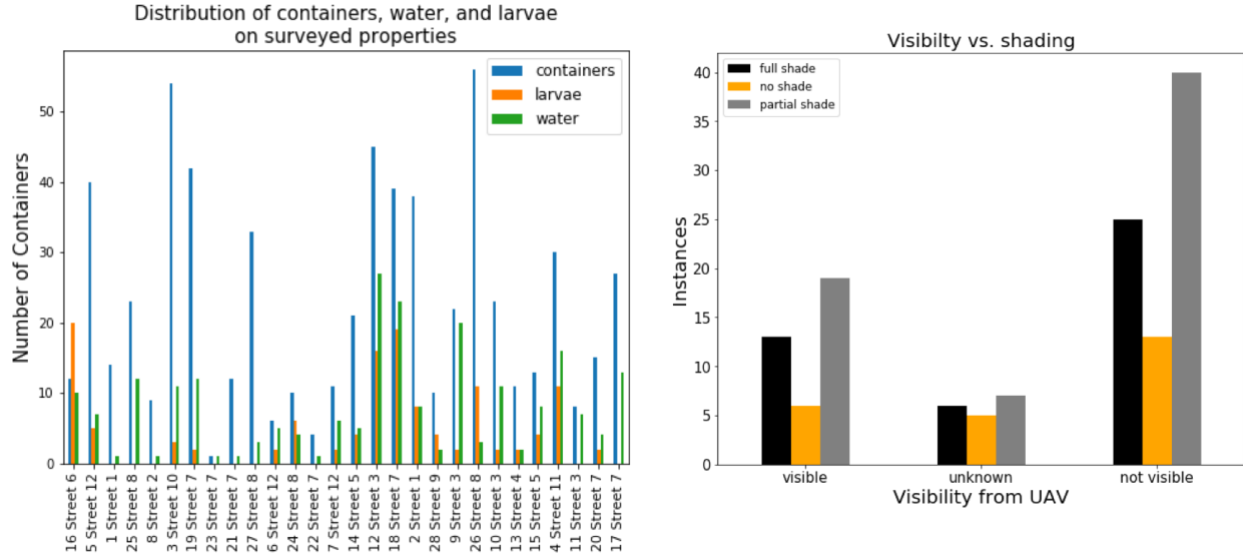


Figure 5: (Left) distribution of containers on anonymized properties. Blue is the total number of containers, orange is the magnitude of larvae and pupae presence (0 – no larvae/pupae, 1 – 1-25 larvae/pupae... 4 – 100+ larvae/pupae) and green is the number of containers that held water. (Right) there was no significant difference between the number of containers that could be seen by the UAV that were in full sun versus shaded (18%) and could not be seen by the UAV in full sun versus shaded (20%)

location), and 18 could not be identified in the aerial photos from notes and pictures on the ground taken during the surveys.

This study also examined the relationship between the number of containers on a property, the number of containers with water, and larval presence. We found a significant linear relationship ($p < 0.01$) between number of containers and number of containers with water and larval presence using the sklearn [29] and Statsmodels [30] python packages; however, we were unable to use a logistic regression to create a binary classifier for larval presence based on the number of containers.

As previous research has shown that *Ae. albopictus* may prefer containers with some shading, we also recorded the amount of shading experienced by each container and whether these could be seen by the UAV. [28] The ratio of shaded to full sun images remained consistent between the sets of containers visible and not visible to the UAV. See Figure 5 for the distribution of all

containers among properties (anonymized with aliases) and the shading of containers in relation to their visibility.

Image Segmentation

On the test dataset, SSD300 successfully identified containers as small as 12 cm in diameter, though not consistently, and with a trade-off between precision, recall and accuracy, as defined in Equations 1, 2 and 3:

$$Precision = \frac{TP}{TP+FP} \quad (\text{Eq. 1})$$

$$Recall = \frac{TP}{TP+FN} \quad (\text{Eq. 2})$$

$$Accuracy = \frac{TP}{TP+FN+FP} \quad (\text{Eq. 3})$$

where TP = true positives (correctly identified containers); FP = false positives (misabeled containers or incorrectly activated on background features); and FN = false negatives (features that were missed).

Part of the difficulty of this problem is the precise definition of container, which creates a category with a vague definition. However, mislabeling was considered less of a problem than recall, especially among similar objects – for example, the broad definition of container, flower pots, pots and small garbage bins may look visually similar. Larger, distinct items, such as cars, were identified with substantial success.

In the sample set, with 1080 tagged images from 12,281 tiled scene images, 810 images were used for training, 162 images were used for validation and 108 were used for testing. Weights from ImageNet [31] were used to initialize the neural network, which was the fine-tuned via transfer learning on our dataset.

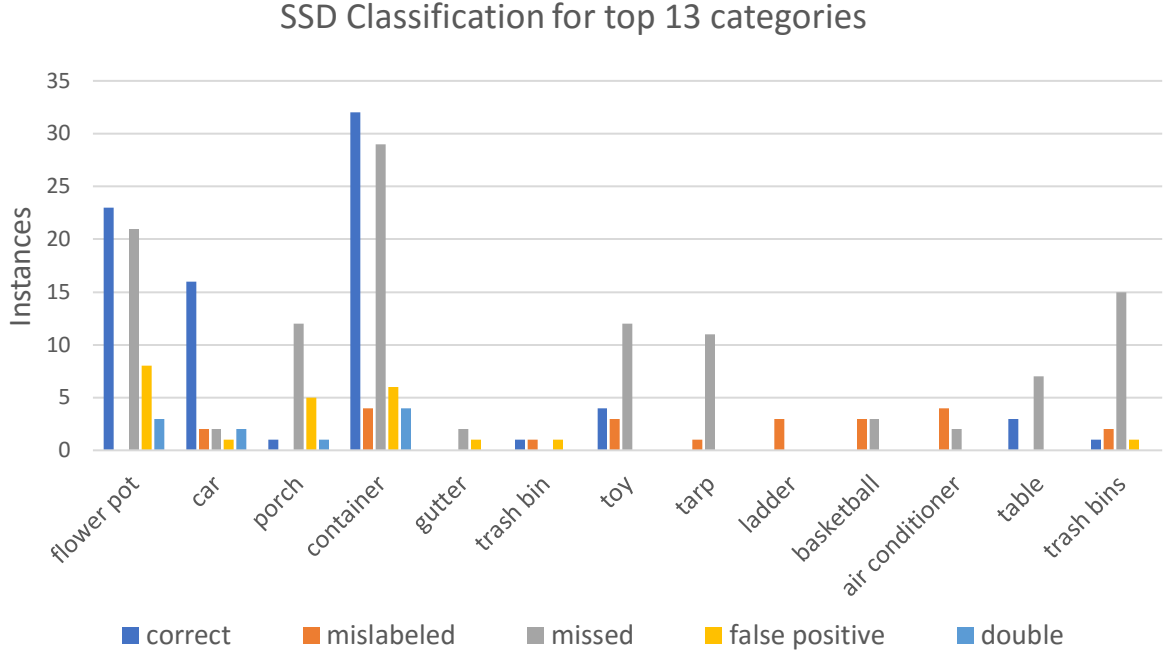


Figure 6: The neural network successfully recalled 35% of the items and correctly identified the items 60% of the time. This was higher for objects that were better represented in the data set, like flower pots, which were identified correctly 100% of the time, and containers, which were identified correctly 90% of the time.

The performance of the test set was evaluated in two ways: 1) by comparing the Jaccard overlap index between neural network output at confidence levels above 0.05 and the ground truth data; and 2) through manual validation. The latter was performed because the authors found that the neural network would identify containers that had been missed during tagging, identify new ones, or categorize an object in a way that could be interpreted as correct. For example, is a roof area used to store items a porch? Is a bucket with a plant in it a flower pot? The Jaccard index is a measure of the similarity between datasets, defined as the intersection over union between the ground truth bounding boxes and the output of the neural network; see Equation 4. See Figure 6 for evaluation of the test set.

$$Jaccard\ index = \frac{|A \cap B|}{|A \cup B|} \quad (Eq. 4)$$

The neural network found 35% of the objects (recall), and correctly identified these 59% of the time (precision). Half of the items were mislabeled as containers; if these are chosen to count as

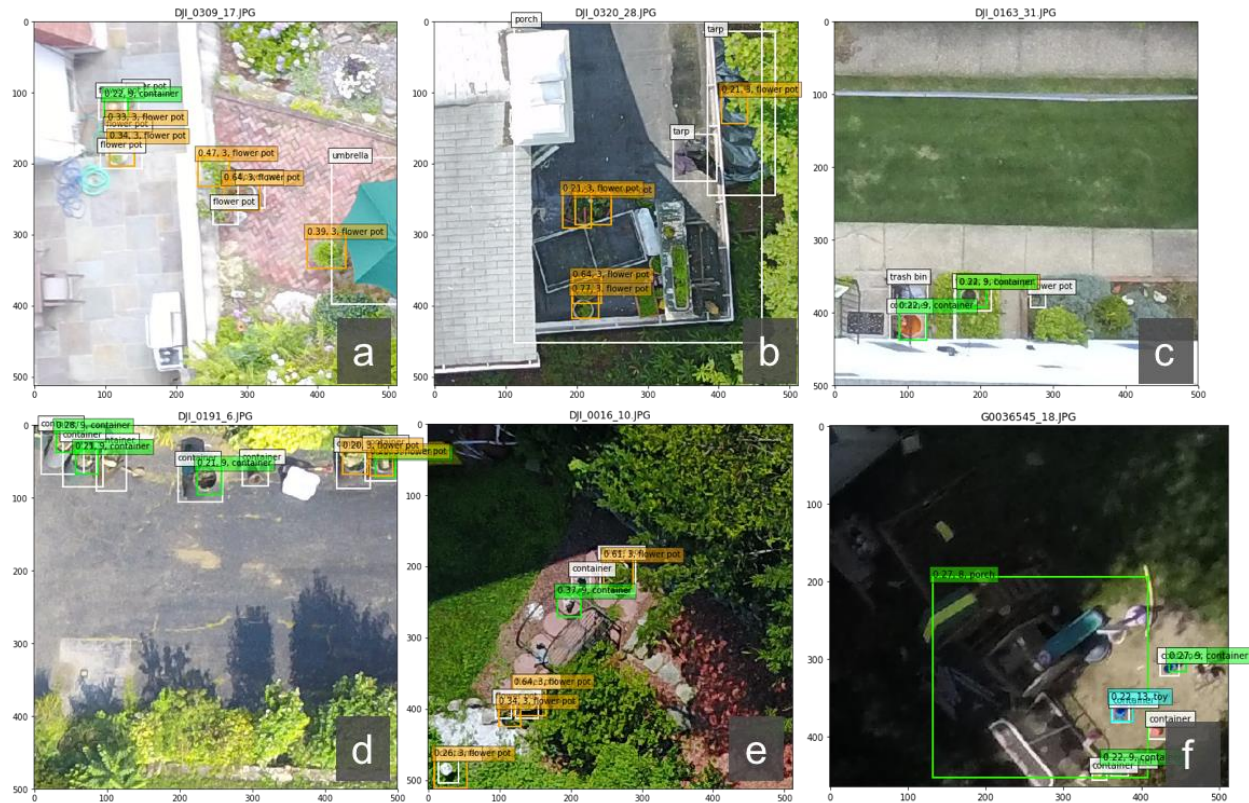


Figure 7: Sample outputs of SSD300. White boxes are ground truth; colored boxes are the neural network. See, in particular, b and f for examples of where the neural network output correct annotations that were not labelled in the annotation set.

successful IDs— a reasonable consideration, since it is a broad and relevant category— the precision improves 8% from 59% to 67%, the recall improves to 40%, and the accuracy to 35% at a minimum confidence level of 0.2. Different features were visible at different confidence levels. See Figure 7 for examples of images produced by the network with correct identifications. The authors investigated the ability of the network to classify containers *in situ* as positive or negative for larvae; however, the sample size was extremely small for these (24 positive, about 50 negative). As a result, no images in the test set included containers that were found to contain larvae. In the validation set, the neural network did not output any positive or negative larvae classifications, indicating that either more data are needed for the network to learn identification, or not enough information is available from visible-light photos to differentiate positive and negative larvae containers.

Binary Classification

Finally, we investigated whether a fully convolutional network based on the architecture of VGG16 could classify whole images as positive or negative for mosquito larvae. Based on [32], we kept and locked the convolutional layers of the VGG16 architecture with pre-computed ImageNet weights, removed the dense layers, and added four convolutional layers, each followed by batch normalization and a max pooling process. We used dropout and global average pooling at the end of the architecture, and softmax for our activation function. Our sample set for this was extremely small, with just 34 properties

positive or negative for larvae. However, some of the activations of the filters were of interest; these could be accessed by examining the neural network output after the global average pooling layer and before the softmax classification. Hot spots – where layers activate the strongest – could potentially provide guidance to vector control personnel for where to look; at the least, they show that the neural network looks at the same locations as a human would for classifying a household (side, front and back yards). This is a technique that should be explored in future work. See Figure 8 for a layer with one of the most significant activations for larval detection.

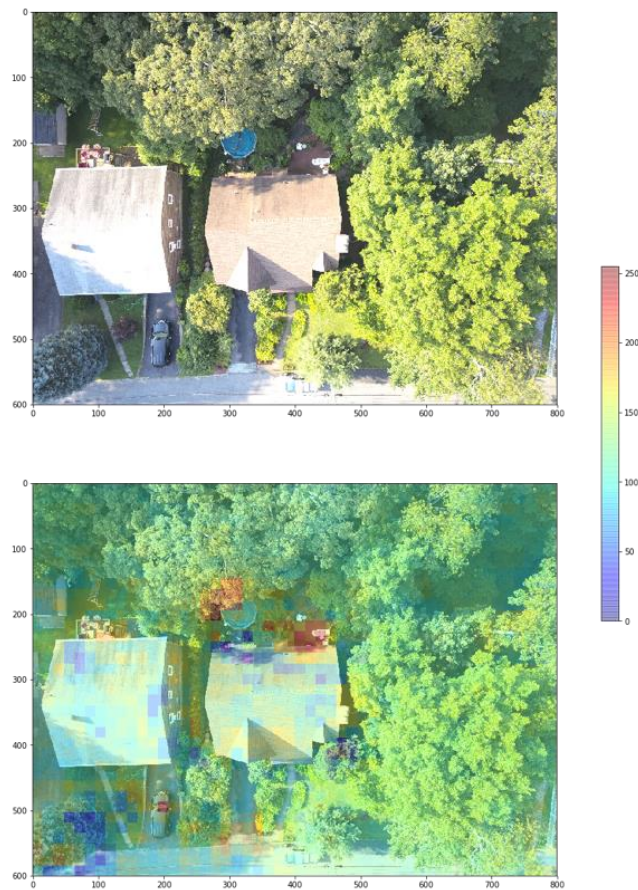


Figure 8: Example of an activation layer of the fully convolutional network, which lights up strongly on the back and front yards (where one would expect to find containers of interest), and particularly, on the porch area where many containers were located. This house was positive for larvae; permission from the owner was obtained from the owner to publish this photograph.

DISCUSSION

Unmanned aerial vehicles were effective at capturing some, but not all, of the containers of interest. In particular, items that were covered by awnings, or under trees or porches, were not visible from above. Additionally, in a residential area it was difficult to comply with Federal Aviation Administration restrictions on when and where UAVs could be flown – particularly, avoiding flying over any person not involved with the flight. The commercial product – the DJI Mavic – was a superior data collection tool and is recommended for future work because it was more stable for higher image quality, had a longer battery life, and collected more information about the headings and GPS locations of the images.

There are two other factors that need to be considered prior to deploying this technology: public engagement and a right to privacy. First, the authors had numerous positive interactions with the public about the use of drones in research. Thus, we recommend that the drones be employed not just as survey tools, but as an opportunity for STEM outreach and citizen science.

Second, there is a clear question of privacy: should government (or private) agencies have easy access to private property, and is it a violation of fourth amendment rights? While public satellites can take photographs at 30 cm resolution, and U.S. government satellites have been used by researchers in polar regions for their 5-10 cm resolution images, drones democratize and cheapen access to this kind of potentially private and personal information. So far, there is no legal precedent prohibiting the use of drones to collect information about backyards; however, some states have general “reasonable expectation of privacy” laws that may conflict with data collection. Finally, the FAA restricts flight over people, which could make the collection of data in populated areas impractical. We therefore recommend that if vector control agencies decide to use UAVs in populated areas to monitor mosquito habitat, that they create a document of best

practices (including, for example, blurring personal information like license plates and faces) and hold town halls to inform and engage local citizens about these efforts prior to data collection. Still, used responsibly, this technique could prove a formidable tool for monitoring mosquito population and efficiently identifying houses for control measures. Future work could include larval surveys that use the output of the neural network as a determinant for choosing houses to survey, and combining the outputs of the fully convolutional network and SSD for a more comprehensive, top-down, bottom-up classification scheme.

CONCLUSION

This paper investigated the use UAVs to capture images of suburban mosquito habitat, and the ability of an image segmentation neural network to classify features of interest within these photographs.

From more than 12,000 tiled photographs, more than 2500 features of interest were tagged on 125 properties in southern New York. This is the first dataset, to the authors' knowledge, to investigate the use of neural networks on UAV imagery in suburban neighborhoods. Overall, the network recalled about 40% of the objects and accurately classified them 60% of the time.

Despite Liu, et. al's concerns about SSD300 performance on small objects, classification was precise for objects that were well or over-represented in the training set – for example, flower pots and containers, which dominated the training set, were classified correctly 88-100% of the time.

Some refinement is needed to understand how many containers need to be identified, both by the UAV and the neural network, for this technology to be more useful for vector control agencies. Nevertheless, these tools show promise for expanding the scope of vector control within suburban habitats. Integrated mosquito management could use UAVs and neural networks as

either 1) a preliminary survey tool to identify houses with the most containers or 2) monitor the effectiveness of water dumping campaigns. Future research could improve the usefulness of these tools by incorporating more data for better image recognition and investigating the relationship between the identified containers and appearance of larvae.

REFERENCES

1. Shragai, T., Tesla, B., Murdock, C., & Harrington, L. Zika and Chikungunya: mosquito-borne viruses in a changing world. *Annals of the New York Academy of Sciences*. 2017. doi: 10.1111/nyas.13306
2. Weaver, S., & Reisen, W. Present and future arboviral threats. *Antiviral Research*. 2010; 85(2), 328-345.
3. Roseboom L. E., Rosen L. and Ikeda J. Observations on oviposition by *Aedes (S) albopictus* Skuse and *A. (S) polynesiensis* marks in nature. *J. med. Ent.* 1973; 10, 397–399 <https://doi.org/10.1093/jmedent/10.4.397>
4. Bonizzoni, M., Gasperi, G., Chen, X., James, A.A. The invasive mosquito species *Aedes albopictus*: current knowledge and future perspectives. *Trends in Parasitology*. 2013. doi: 10.1016/j.pt.2013.07.003
5. West Nile Virus in the United States: Guidelines for Surveillance, Prevention, and Control. Centers for Disease Control and Prevention. 2013. <https://www.cdc.gov/westnile/resources/pdfs/wnvguidelines.pdf> Accessed November 25, 2017.
6. Fonseca, D. M., Unlu, I., Crepeau, T., Farajollahi, A., Healy, S. P., Bartlett-Healy, K., Strickman, D., Gaugler, R., Hamilton, G., Kline, D. and Clark, G. G. Area-wide management of *Aedes albopictus*. Part 2: Gauging the efficacy of traditional integrated pest control measures against urban container mosquitoes. *Pest. Manag. Sci.* 2013; 69: 1351–1361. doi:10.1002/ps.3511
7. Meola, A. Drone Industry Analysis: market trends and growth forecasts. Business Insider. 2017. <http://www.businessinsider.com/drone-industry-analysis-market-trends-growth-forecasts-2017-7> Accessed August 6, 2017.
8. Seymour, A. C., Dale, J., Hammill, M., Halpin, P. N., & Johnston, D. W. Automated detection and enumeration of marine wildlife using unmanned aircraft systems and thermal imagery. *Sci Rep*. 2017. doi: 10.1038/srep45127
9. Candiago, S., Remondino, F. De Giglio, M. Dubbini, M., Gattelli, M. Evaluating Multispectral Images and Vegetation Indices for Precision Farming Applications from UAV Images. *Remote Sens*. 2015. doi:10.3390/rs70404026
10. Hardy, A., Makame, M., Cross, D., Majambere, S., & Msellem, M. Using low-cost drones to map malaria vector habitats. *Parasites & Vectors*. 2017. doi: 10.1186/s13071-017-1973-3
11. Suppressing Agricultural Pests with Drones. DJI. 2017. <http://enterprise.dji.com/news/detail/suppressing-agricultural-pests-with-drones>. Accessed July 2017
12. FAA Authorizes Drone Use for Mosquito Control in Florida Keys. Associated Press. 2015. <https://www.nbcmiami.com/news/local/FAA-Authorizes-Drone-Use-for-Mosquito-Control-in-Florida-Keys-287336931.html> Accessed August 6, 2017.
13. Mussallam, A. Drones Being Used To Target Mosquitoes In Placer County. CBS Sacramento. 2017. <http://sacramento.cbslocal.com/2017/04/14/drones-mosquito-control-placer-county/> Accessed August 6, 2017.
14. Prasad, M. G., A. Chakraborty, R. Chalasani, and S. Chandran. “Quadcopter-Based Stagnant Water Identification.” Fifth National Conference on Computer Vision, Pattern Recognition,

- Image Processing and Graphics (NCVPRIPG). 2015; doi:10.1109/NCVPRIPG.2015.7490049.
15. Bernard Widrow and Tedd Hoff. "An adaptive "ADALINE" neuron using chemical "memistors". 1960. <http://www.isl.stanford.edu/~widrow/papers/t1960anadaptive.pdf>
 16. Esteva, A., Kuprel, B., Ko, J., Swetter, S., Blau, H., & Thrun, S. Dermatologist-level classification of skin cancer with deep neural networks. *Nature*. 2017; 542(7639), 115-118.
 17. Hu, F., Xia, G.-S., Hu, J., & Zhang, L. Transferring Deep Convolutional Neural Networks for the Scene Classification of High-Resolution Remote Sensing Imagery. *Remote Sensing*. 2015; 7(11), 14680-14707.
 18. Liu, W., Anguelov, D., Erhan, D., Szegedy, C., Reed, S., Fu, C.-Y., & Berg, A. C. SSD: Single Shot Multibox Detector. *European Conference on Computer Vision*. 2016
 19. K. Simonyan, A. Zisserman. Very Deep Convolutional Networks for Large-Scale Image Recognition. *ArXiv*. 2015. arXiv:1409.1556
 20. Redmon, J. Divvala, S., Girshick, R., Farhadi, A. You Only Look Once: Unified, Real-Time Object Detection. 2016. arXiv:1506.02640
 21. Sermanet, P., Eigen, D., Zhang, X., Mathieu, M., Fergus, R., LeCun Y. OverFeat: Integrated Recognition, Localization and Detection using Convolutional Networks. 2014. arXiv:1312.6229
 22. Summary of small unmanned aircraft rule (part 107). 2016. https://www.faa.gov/uas/media/Part_107_Summary.pdf. Accessed July 2016.
 23. Seys, R. PhotoGPS. Github Repository. 2016. <https://github.com/ryanseys/photogps> Accessed November 2017.
 24. Tzutalin. LabelImg. Github Repository. 2015. <https://github.com/tzutalin/labelImg> Accessed November 2017.
 25. Rykov, A. Port of Single Shot MultiBox Detector to Keras. Github Repository. 2017. https://github.com/rykov8/ssd_keras Accessed November 2017.
 26. Fast.ai AMI link
 27. Diederik P. Kingma, J. B. Adam: A Method for Stochastic Optimization. 3rd International Conference for Learning Representations. 2015. arXiv:1412.6980v9
 28. Citation about shading & albopictus
 29. Pedregosa et al. [Scikit-learn: Machine Learning in Python](#). *JMLR* 12, 2011; pp. 2825-2830
 30. Seabold, S., Perktold, J. "[Statsmodels: Econometric and statistical modeling with python](#)." *Proceedings of the 9th Python in Science Conference*. 2010.
 31. Olga Russakovsky*, Jia Deng*, Hao Su, Jonathan Krause, Sanjeev Satheesh, Sean Ma, Zhiheng Huang, Andrej Karpathy, Aditya Khosla, Michael Bernstein, Alexander C. Berg and Li Fei-Fei. (* = equal contribution) ImageNet Large Scale Visual Recognition Challenge. *IJCV*, 2015.
 32. Howard, J. and Thomas, R. Exotic CNN architectures; RNN from scratch. Fast.ai; 2016. <http://course.fast.ai/lessons/lesson7.html>

APPENDIX

1. Construction of the drone

All parts excluding the Go Pro could be purchased for <\$500. The propellers, motor rpms, electronic speed controllers, and battery were optimized for longer flight time using eCalc. All software and hardware used in this project with the exception of a few specific parts of the drone were open source.

- a. Flight controller: Pixhawk (3DR, Berkeley, CA)
- b. Motors: Multistar Elite 2810 (750 rpm)
- c. Propellers: 1045 and 9045
- d. Electronic speed controllers: Turnigy
- e. Battery: Turnigy (4s, 45C, 6200 mah) and Gens ace (4s, 40C, 3300 mah)
- f. GPS: 3DR (3DR, Berkeley, CA)
- g. Telemetry: 3DR (3DR, Berkeley, CA)
- h. Transmitter and receiver: Taranis and Taranis X8R

2. Data Sheet

MosquitoNet Project								Fieldwork Session #							
Date:		Site:						all measurements in cm							
House #	Street	Type/Mat.	Water?	Visible from drone?	Plants?	Picture taken?	Yard?	Container #	Width	Length	Diam.	Height	# Larvae	# Pupae	Notes
								V only record if water is present V							
Materials: A. Plastic B. Metal C. Rubber D. Ceramic E. Stone/cement F. Natural G. Other Types: 1. Bucket 2. Planter dish 3. Tarp 4. Sheeting 5. Tire 6. Trash 7. Toy 8. Bird bath 9. Piping/tubing 10. Other Water? Y=water in container N = no water in container Visible from drone: V = fully visible P = partially visible N = not visible Picture taken? Y = picture taken N = no picture taken Yard? F = front yard B = back yard Plants: N=no plants =live plants D=dead plants LD=live and dead plants # Larve/pupae: 0-25, 25-50, 50-100, >100								Note - match container number with entomologists							

3. Full Collection of Items Tagged in UAV Photographs

{“background”, “car”, “trash”, “woodpile”, “table”, “tire”, “fence”, “air conditioner”, “flower pot”, “porch”, “house”, “kayak”, “front yard”, “toy”, “bench”, “flower bed”, “driveway”, “yard”, “street”, “pool”, “chair”, “tarp”, “bird bath”, “container”, “back yard”, “gutter”, “trash bin”, “fire pit”, “air conditioner”, “umbrella”, “treehouse”, “basketball”, “tent”, “hose”, “drain”, “barbecue”, “awning”, “fountain”, “bucket”, “ladder”, “toy”, “clutter”, “stone feature”, “larvae”, “no larvae”}